

liquid also, in the sense that sometimes the first step only was found, or the first and the third but not the second.

Very recently, measurements of mobility in liquid helium at 1.14°K have been reported by Schwarz,<sup>17</sup> without evidence of steps. He measured with a method which is practically the same as the present one, and ascribes the steps to spurious effects due to the method used previously.<sup>1,3,4</sup> We think that it seems very unlikely that an effect of the method could give results simply related to the normal superfluid densities<sup>4</sup> and radically different below and above the  $\lambda$  point.<sup>18</sup> Moreover, the present results and those reported by Henson<sup>6</sup> rule out any explanation of the disagreement in terms of trival spurious effects due to the method of measurement.

\*Work supported by Consiglio Nazionale delle Ricerche.

<sup>1</sup>G. Careri, S. Cunsolo, and P. Mazzoldi, Phys. Rev. Lett. **7**, 151 (1961), and Phys. Rev. **136**, A303 (1964).

<sup>2</sup>G. Careri, S. Cunsolo, and M. Vicentini Missoni, Phys. Rev. **137**, A311 (1964).

<sup>3</sup>J. A. Cope and P. W. F. Gribbon, in *Proceedings of the Ninth International Conference on Low Temperature Physics, Columbus, Ohio, 1964*, edited by J. C. Daunt, D. O. Edwards, F. J. Milford, and M. Yaquib (Plenum, New York, 1964), p. 153, and Phys. Lett. **16**, 128

(1965), and J. Phys. C: Proc. Phys. Soc., London **3**, 460 (1970).

<sup>4</sup>L. Bruschi, P. Mazzoldi, and M. Santini, Phys. Rev. Lett. **17**, 292 (1966), and Phys. Rev. **167**, 203 (1967).

<sup>5</sup>D. L. Goodstein, V. Buontempo, and M. Cerdonio, Phys. Rev. **171**, 181 (1968).

<sup>6</sup>B. L. Henson, Phys. Rev. **135**, A1002 (1964), and Phys. Rev. Lett. **24**, 1327 (1970).

<sup>7</sup>K. Huang and A. C. Olinto, Phys. Rev. **139**, A1441 (1965).

<sup>8</sup>C. Di Castro, Nuovo Cimento **42**, 251 (1966).

<sup>9</sup>L. Bruschi, P. Mazzoldi, and M. Santini, Phys. Rev. Lett. **21**, 1738 (1968).

<sup>10</sup>L. Bruschi and M. Santini, Rev. Sci. Instrum. **41**, 102 (1970). In this paper, p. 104, Ref. 5, we reported also that we found steps in liquid nitrogen.

<sup>11</sup>Società Italiana Ossigeno, Milano, Code UPP. Purity 99.999%.

<sup>12</sup>Società Italiana Ossigeno, Milano, Code UPP. Purity 99.995%.

<sup>13</sup>Carlo Erba Company, Milano, Code RS, No. 434697.

<sup>14</sup>I. Ademczewski, *Les Phénomènes d'ionization et de Conduction dans les Dielectriques Liquides* (Masson et Cie., Paris, 1968).

<sup>15</sup>V. Essex and P. E. Secker, Brit. J. Appl. Phys. **2**, D1107 (1969).

<sup>16</sup>S. Cunsolo, Nuovo Cimento **21**, 76 (1961).

<sup>17</sup>K. W. Schwarz, Phys. Rev. Lett. **24**, 641 (1970).

<sup>18</sup>See Fig. 5 of the second paper of Ref. 4. The two sets of measurements were made with the same apparatus, the same method, in the same range of drift velocity, with low field mobilities differing only by 15%.

## THEORY OF STRUCTURE IN THE SUPERFLUID HELIUM SPECTRUM CONSIDERING ROTON-ROTON RESONANCES\*

J. Ruvalds and A. Zawadowski†

Department of Physics, University of Virginia, Charlottesville, Virginia 22901

(Received 2 June 1970)

Interactions between excitations in superfluid helium are investigated by Green's function techniques. In our model, a sharp peak appears in the two-excitation spectrum corresponding to a resonance of two rotons. Interaction of the resonance with the single-particle spectrum results in a hybridization and splitting of the one-particle spectrum into two distinct branches. These theoretical results are in agreement with recent neutron-scattering and Raman-scattering experiments.

The excitation spectrum of superfluid He<sup>4</sup> has attracted considerable interest in the last thirty years following the pioneering work of Landau.<sup>1</sup> Recent developments in experimental techniques have made possible the observation of anomalous structure in the energy spectrum with reasonable accuracy. The aim of the present work is to explain some of these anomalies as a result of the roton-roton interaction.

Recent neutron-scattering experiments<sup>2</sup> have exhibited two particularly strange features which

are shown in Fig. 1(a) by the solid lines: (a) the peculiar flatness of the spectrum for large momenta ( $K < 2k_0$ ) at an energy approximately equal to twice the single roton energy, and (b) the existence of another branch of the spectrum (for  $K < 2k_0$ ) which is continuously connected to the free helium spectrum at very large momenta ( $K > 2k_0$ ).<sup>2</sup>

The possibility of observing two rotons by neutron scattering was first suggested by Pitaevskii.<sup>3</sup> Later Anderson proposed that the flat part of the spectrum near  $2\Delta$  may be associated with the

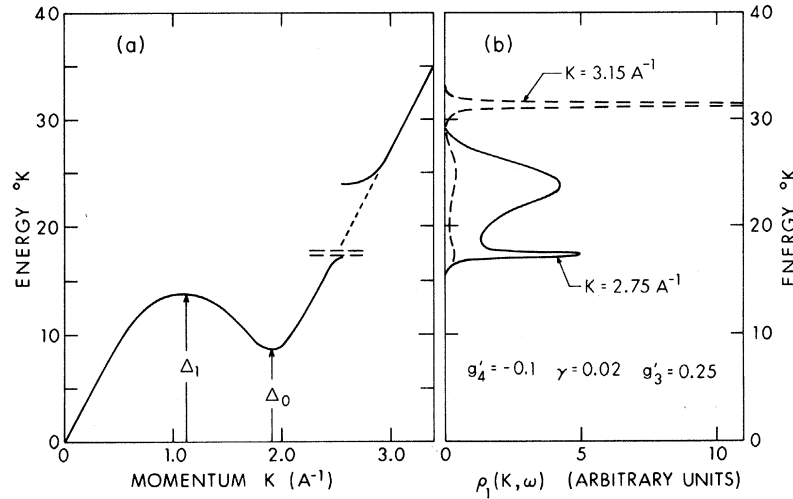


FIG. 1. (a) Dispersion curve for liquid He<sup>4</sup> taken from neutron-scattering data. The double-dashed line corresponds to a two-roton resonance. (b) Single-particle spectrum ρ<sub>1</sub>(K, ε) as a function of energy.

two-roton density of states.<sup>4</sup> However, the spectrum for two independent rotons with large total momentum,  $K \sim k_0$ , does not exhibit a peak. In addition, the Pitaevskii theory of roton-roton interactions does not explain the detailed experimental results discussed above.

To our knowledge there has been no previous theoretical work which considers the splitting of the superfluid helium energy spectrum into two distinct branches.

By means of laser technology Greytak and Yan have succeeded in measuring the portion of the second-order Raman spectrum which is associated with the excitation of two rotons with total momentum  $\vec{K} = \vec{k}_1 + \vec{k}_2 \approx 0$ .<sup>5</sup> The density of states for two noninteracting excitations (with  $\vec{K} = 0$ ) exhib-

its two peaks associated with the minimum and maximum of the dispersion curve [see dotted line in Fig. 2(a)], in contrast to the striking asymmetric experimental results of Ref. 5 which bear a close resemblance to the solid lines in Fig. 2(a). One contribution to the asymmetry of the Raman spectrum may be due to the smooth energy dependence of the Raman efficiency<sup>6</sup> which affects the relative amplitudes of the two peaks, but cannot explain the disappearance of the peak near  $2\Delta_1$  as observed experimentally.<sup>5</sup>

The purpose of the present work is to demonstrate that all of the above mentioned anomalous experimental features can be readily explained on the basis of the formation of two-roton resonances at energies near twice the minimum sin-

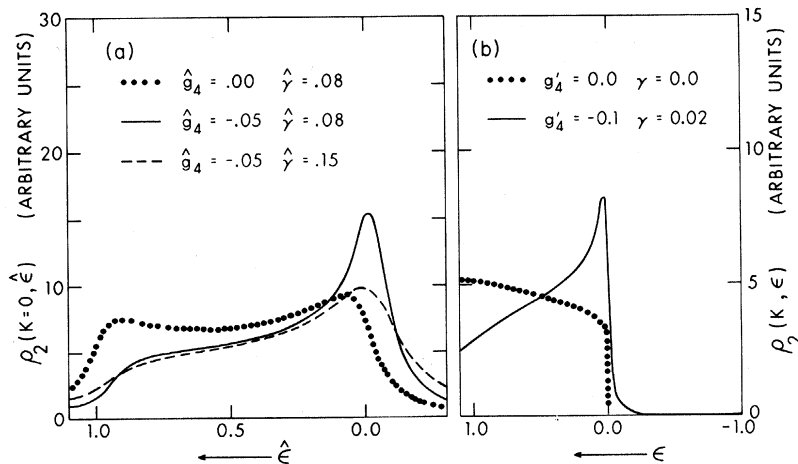


FIG. 2. (a) Two-roton spectral function ρ<sub>2</sub>(K = 0, ε) plotted as a function of energy for different values of the coupling parameters. (b) Unrenormalized two-roton spectrum ρ<sub>2</sub><sup>(0)</sup> with K ≠ 0 (dotted line), and spectrum ρ<sub>2</sub> including roton-roton interactions.

gle-roton energy. We assume a negative roton-roton coupling which shifts the two-roton spectrum to lower energies and results in a large enhancement of the spectrum near  $2\Delta$  for momenta  $K > 0.2 k_0$ . In this momentum region the enhancement gives rise to a sharp peak corresponding to a two-roton resonance. Also, in the case of total momentum  $\vec{K} \approx 0$  the amplitude of the peak in the density of states at lower energies is enlarged while the peak corresponding to the energy maximum is destroyed.

Our theoretical treatment of two-roton resonances is analogous to the theory of bound phonon pairs in crystals.<sup>7</sup> It is interesting to note that some of the experimental results for superfluid helium display features which are similar to structure observed in the Raman spectrum of insulators.<sup>8</sup>

Our theory is based on the model Hamiltonian

$$\mathcal{H} = \mathcal{H}_0 + \frac{1}{2}g_4 \int \psi^\dagger(x)\psi^\dagger(x)\psi(x)\psi(x)dx, \quad (1)$$

where  $\mathcal{H}_0$  is identified with the excitation spectrum shown by dotted lines in Fig. 1(a), and  $\psi(x)$  is the usual helium field operator.<sup>9</sup> The interaction between excitations is described by the phenomenological coupling constant  $g_4$  which corresponds to the irreducible two-excitation vertex function. The momentum dependence of the vertex function is assumed to be smooth and may result in different values of the coupling at various regions of the spectrum. Contributions from the condensed zero-momentum particles can be removed by introducing field operators  $\psi' = \psi - \xi_0$ , as discussed in Ref. 9. To calculate the one- and two-particle spectrum we introduce the Green's functions:

$$G_1(x-x') = -i \langle T[\psi'(x)\psi'^\dagger(x')] \rangle;$$

$$G_2(x-x') = -i \langle T[\psi'(x)\psi'(x)\psi'^\dagger(x')\psi'^\dagger(x')] \rangle. \quad (2)$$

We employ zero-temperature techniques, since we are interested in the high-energy part of the spectrum at very low temperatures. For small temperatures, the main contribution to the scattering of excitations is from diagrams containing two-roton intermediate states as shown in Fig. 3(a).

In the definition of the Fourier transform of the single-particle propagator, i.e.,  $G_1^{-1}(\vec{k}, \omega) = \omega - \epsilon_k + i\Gamma/2$ , a phenomenological one-particle lifetime  $\Gamma^{-1}$  is introduced and is considered to be temperature dependent. Furthermore, the unrenormalized  $\epsilon_k$  is approximated by  $\epsilon_k^\alpha = \Delta_\alpha + (k-k_\alpha)^2/(2\mu_\alpha)$ , where  $\alpha=0$  refers to rotons, and  $\alpha=1$  designates excitations near the energy maximum (with effective mass  $\mu_1 < 0$ ).

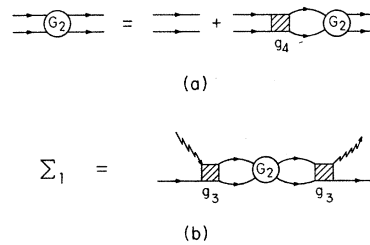


FIG. 3. (a) Bethe-Salpeter equation for two-roton propagator  $G_2$ . (b) Dyson equation for single-particle self-energy  $\Sigma_1$ .

imum (with effective mass  $\mu_1 < 0$ ). The meaning of the parameters  $\Delta_0$ ,  $\Delta_1$ ,  $k_0$ , and  $k_1$  is clear from Fig. 1(a). Using the above approximations, a straightforward calculation yields  $G_2(K, \omega) = 2F(K, \omega)/[1 - g_4 F(K, \omega)]$ , where  $F(K, \omega)$  is defined by

$$F(K, \omega) = \frac{i}{(2\pi)^4} \int d^3k \int d\tilde{\omega} G_1(K-k, \omega-\tilde{\omega}) G_1(k, \tilde{\omega})$$

$$= 2 \int \frac{\rho_2^{(0)}(K, \omega')}{\omega - \omega' + i\Gamma} d\omega', \quad (3)$$

where we have introduced the spectral function

$$\rho_2^{(0)}(k, \omega) = \frac{i}{2(2\pi)^3} \int d^3k \delta(\omega - \epsilon_k - \epsilon_{K-k}). \quad (4)$$

That is,  $\rho_2^{(0)}$  is simply the unrenormalized two-excitation spectrum in the case where our phenomenological one-particle lifetime  $\Gamma$  is taken to approach zero.

First we consider the Raman scattering process and therefore take  $K = 0$ . In this case one obtains,<sup>6</sup> for energies  $2\Delta_0 < \omega < 2\Delta_1$ ,

$$\rho_2^{(0)}(K=0, \omega) = \left(\frac{k_0}{2\pi}\right)^2 \left(\frac{\mu_0}{\omega - 2\Delta_0}\right)^{1/2}$$

$$+ \left(\frac{k_1}{2\pi}\right)^2 \left(\frac{\mu_1}{2\Delta_1 - \omega}\right)^{1/2}. \quad (5)$$

Introducing dimensionless quantities  $\hat{\epsilon} = (\omega' - 2\Delta_0)/(2D)$ ,  $\hat{\gamma} = \Gamma(2D)^{-1}$ , and  $\hat{\eta} = k_0\pi^{-2}(\mu_0/2D)^{1/2}$ , where  $D = \Delta_1 - \Delta_0$ , Eq. (3) takes the form  $F(K, \omega) = \frac{1}{2}\hat{\eta}\hat{f}(\hat{\epsilon}, \hat{\gamma})$ , and  $G_2$  becomes

$$G_2(K=0, \omega) = \hat{\eta} \frac{\hat{f}(\hat{\epsilon}, \hat{\gamma})}{1 - \hat{g}_4 \hat{f}(\hat{\epsilon}, \hat{\gamma})}, \quad (6)$$

where the dimensionless coupling constant is  $\hat{g}_4 = \hat{\eta}g_4/2$ , and  $\hat{f}$  can be evaluated numerically. The density of states is given by  $\rho_2(K, \omega) = -(4\pi)^{-1} \times \text{Im}G_2$ .

Raman scattering experiments measure the density of states  $\rho_2(K=0, \omega)$ . We display in Fig. 2 the striking modifications of the density of states

due to interactions between excitations. These results are characterized by a coupling  $\hat{g}_4 = -0.05$  and various values of the single excitation widths  $\hat{\gamma}$ . From the figure it is apparent that (a) the higher energy peak in the unrenormalized spectrum is completely smeared out by the  $\hat{g}_4$  coupling, and (b) the low-energy peak is enhanced, forming a two-roton resonance, and is shifted slightly in energy. The singularities in the unperturbed density of states are removed by the single-particle width  $\hat{\gamma}$ . The ratio of the peaks is primarily determined by the value of  $\hat{g}_4$ . The calculated spectrum  $\rho_2$  in Fig. 2 shows a remarkable resemblance to the experimental results of Greytak. A detailed fit to the experiment can be carried out using the present formalism, and should yield accurate values for the roton lifetimes when the experimental uncertainty due to instrumental width is reduced.

The formation of a two-roton resonance with momentum  $K \neq 0$  is especially spectacular since the unrenormalized two-roton density of states has no peaks in the momentum interval of interest ( $\frac{1}{2}k_0 < K < 2k_0$ ), as can be seen from a straightforward evaluation of Eq. (4) which gives

$$\rho_2^{(0)}(K, \omega) = (8\pi^2 K)^{-1} \mu_0 [\pi k_0^2 + 2k_0 \mu_0^{1/2} (\omega - 2\Delta_0)^{1/2}], \quad (7)$$

with  $\omega > 2\Delta_0$ . The spectrum  $\rho_2^{(0)}(K, \omega)$  is shown by dotted lines in Fig. 2(b). By inserting the density of states from Eq. (7) into Eq. (6), the resulting spectrum can be expressed in terms of "hatless" dimensionless quantities  $\epsilon = (\omega - 2\Delta_0)/\Delta_0$ ,  $\epsilon' = (\omega' - 2\Delta_0)/\Delta_0$ , and  $\gamma = \Gamma/\Delta_0$ . As before, one obtains  $F(K, \omega) = \eta f(\epsilon, \gamma)$  with  $\eta = \mu_0 k_0^2 / (4\pi K)$ .

Finally the relevant dimensionless coupling constant is given by  $g_4'(K) = \eta g_4$ . In the latter calculation the relevant functions [Eq. (5)] can be obtained by simply omitting the "hat" marks.

The results for the two-roton resonance with  $K \neq 0$  are shown in Fig. 2(b). For this calculation, the single roton width was taken to be of the same order as in the  $K = 0$  spectrum. Therefore the effect of the roton-roton interaction is to produce a large peak in the two-roton spectrum as seen in Fig. 2(b).

If we limit the neutron-scattering cross section to include only single excitation processes, then the two-roton resonance cannot be directly observed. However, a single excitation accompanied by a boson from the condensed state can be transformed into two rotors. In that way, there is a direct interaction between single-particle

excitations and the two-roton resonance. As illustrated in Fig. 1(a), when the single-particle spectrum intersects the two-roton resonance (at  $K \approx 1.5k_0$ ) a hybridization process can occur. Therefore, the two-roton resonance structure will be manifested in the single-particle spectrum. The hybridization process can be treated by the model Hamiltonian

$$\mathcal{H}^{(3)} = g_3 \int \psi'^{\dagger}(x) \psi'^{\dagger}(x) \psi'(x) \xi_0 N_0^{-1/2}(T) + \text{c.c.}, \quad (8)$$

which can be derived from the Hamiltonian in Eq. (1) by taking the coupling as  $g_3 = g_4 N_0^{1/2}(T)$ , where the creation or annihilation operators of the condensed bosons  $\xi_0$  are replaced by the  $c$ -number  $N_0^{1/2}$ ;  $N_0(T)$  is the number of condensed bosons in the system. The contribution of the two-roton resonance to the one-particle self energy is given diagrammatically in Fig. 3(b).

A direct evaluation of the expression for the self-energy  $\Sigma_1$  and subsequent substitution into the single-particle propagator gives

$$G_1(K, \omega) = \frac{1}{\Lambda_0} \left[ \epsilon - \Omega_K + i \frac{\gamma_K}{2} - (g_3')^2 \frac{f(\epsilon, \gamma)}{1 - g_4'(K) f(\epsilon, \gamma)} \right]^{-1}, \quad (9)$$

with a dimensionless coupling constant  $g_3'(K) = g_3(\eta/\Delta_0)^{1/2}$ ;  $\Omega_K = (\epsilon_K - 2\Delta_0)/\Delta_0$  is the dimensionless one-particle energy, and  $\gamma_K = \Gamma_K/\Delta_0$  is a phenomenological single-particle width which does not contain contributions of the  $g_3$  coupling. Then it is clear from Eq. (9) that the two-roton resonance will distort the one-particle density of states  $\rho_1(K, \omega) = -\pi^{-1} \text{Im} G_1(K, \omega)$ .

The above hybridization process results in a mixing of single excitation branches with the two-roton resonance. Thus the one-excitation spectral function  $\rho_1(K, \omega)$ , exhibits now two peaks near the hybridization point. This hybridization process is illustrated in Fig. 1(b), where we have taken  $\gamma_K = 0$  to illustrate solely the hybridization process. However, it should be noted that the partial width  $\gamma_K$  is in fact responsible for the large broadening of the single-particle spectrum with increasing momentum. Note that the maxima of the peaks in  $\rho_1(K, \omega)$  correspond to the solid lines in Fig. 1(a). The relative amplitudes and line shapes of the peaks are presented for representative momentum values in Fig. 1(b). Coupling values of  $g_3'$  were chosen to give peaks of comparable strength. At large  $K$  values the upper energy curves are dominated by single-

particle excitations, consequently the spectral weight of the resonance reduces to a small portion of the total spectrum. On the other hand, for smaller values of  $K \sim k_0$ , the peak intensity ratios are inverted. It is worth mentioning that the sum rules for the total spectral intensity must be exactly satisfied, i.e.,  $\int \rho(\omega) d\omega = 1$ . Lastly, it is interesting to note that the coupling  $g_3$  and the hybridization process vanish as the number of condensed bosons  $N_0$  tends to zero.

As the limit  $K \geq 2k_0$  is approached, the minimum energy of two independent rotons is larger than  $2\Delta$ , and the energy of the resonance should increase with larger total momentum.

By neutron-scattering measurements, the spectral function of the density-density correlation function  $S(K, \omega)$  is observed, which, in the case of Bose condensation, is strongly related to the one-excitation spectral function  $\rho_1(K, \omega)$ . This means that the structure appearing in  $\rho_1(K, \omega)$  is also exhibited by  $S(K, \omega)$ .<sup>10</sup>

In all of our results for the excitation spectrum, values of the parameters were chosen to give reasonable agreement with existing experimental data. These parameters yield the following estimates for the coupling  $g_4$  (erg cm<sup>3</sup>): (a)  $\hat{g}_4 = -0.05 \rightarrow g_4 = -1.0 \times 10^{-39}$ , (b)  $g_4' = -0.1 \rightarrow g_4 = -1.4 \times 10^{-39}$ , (c)  $g_3' = 0.25 \rightarrow |g_4| \sim 5 \times 10^{-39}$ , (d)  $\hat{\gamma} = 0.15 \rightarrow |g_4| \sim 3 \times 10^{-39}$ . The values of  $g_4$  derived from the dimensionless constants used above are all of the same order of magnitude. Since the coupling is related to a vertex function with momenta in different regions, such deviations are expected.

There are two previous estimates of the roton-roton scattering strength. Khalatnikov,<sup>11</sup> on the basis of viscosity data, finds  $|g_4| = 1.87 \times 10^{-38}$  erg cm<sup>3</sup>. Secondly, Cohen and Feynman have supposed that the dominant contribution to the roton-roton scattering comes from the process of one roton emitting a phonon which is absorbed by another roton. The latter mechanism gives an attractive roton-roton interaction in agreement with our assumption, and is estimated for small momentum exchange to be  $g_4 = -1.3 \times 10^{-38}$  cm<sup>3</sup>.<sup>10</sup>

We conclude, on the basis of the assumption that the roton-roton interaction is attractive,

that a two-roton resonance can be formed in a wide region of momentum space. Such a state explains the anomalous features of the Raman-scattering data and the structure of the dispersion curve observed by neutron scattering.

We are very grateful to Professor T. Greytak for valuable discussions of his data and especially for calling our attention to the existence of two branches in the dispersion curve. Numerous discussions with Professor V. Celli have been most helpful.

---

\*Research supported by the Center for Advanced Studies at the University of Virginia.

†Permanent address: Central Research Institute for Physics, Budapest, Hungary.

<sup>1</sup>L. D. Landau, J. Phys. USSR **5**, 71 (1941), and **11**, 91 (1947). References to more recent work can be found in, e.g., R. J. Donnelly, *Experimental Superfluidity*, (Univ. of Chicago, Chicago, Ill., 1967).

<sup>2</sup>A. D. B. Woods, in *Quantum Fluids*, edited by D. F. Brewer (North-Holland, Amsterdam, 1966), p. 242; A. D. B. Woods and R. A. Cowley, in *Proceedings of the Symposium on Neutron Inelastic Scattering, Copenhagen, Denmark, 1968* (International Atomic Energy Agency, Vienna, Austria, 1968).

<sup>3</sup>L. P. Pitaevskii, Zh. Eksp. Teor. Fiz. **36**, 1168 (1959) [Sov. Phys. JETP **9**, 830 (1959)].

<sup>4</sup>This suggestion was made in a discussion in the Sussex University Symposium on Quantum Fluids; see Woods, Ref. 2, p. 255.

<sup>5</sup>T. J. Greytak and J. Yan, Phys. Rev. Lett. **22**, 987 (1969). The possibility of observing rotons by Raman scattering was suggested by J. W. Halley, Phys. Rev. **181**, 338 (1969).

<sup>6</sup>M. J. Stephen, Phys. Rev. **187**, 279 (1969). The analogous scattering in solid helium has been considered by N. R. Werthamer, Phys. Rev. **185**, 348 (1969).

<sup>7</sup>M. H. Cohen and J. Ruvalds, Phys. Rev. Lett. **23**, 1378 (1969); J. Ruvalds and A. Zawadowski, Phys. Rev. B (to be published).

<sup>8</sup>See, for example, J. F. Scott, Phys. Rev. Lett. **21**, 907 (1968), and references cited therein.

<sup>9</sup>A. A. Abrikosov, L. P. Gor'kov, and I. E. Dzyaloshinski, *Methods of Quantum Field Theory in Statistical Physics*, edited by R. Silverman (Prentice-Hall, Englewood Cliffs, N. J., 1963).

<sup>10</sup>M. Cohen and R. P. Feynman, Phys. Rev. **107**, 13 (1957).

<sup>11</sup>I. M. Khalatnikov, *Introduction to the Theory of Superfluidity* (Benjamin, New York, 1965).